Radiation-induced cellular senescence in salivary glands

Peng, Julie

DOI:
10.33612/diss.103407924

Chapter 4

GDNF – a marker for radiation induced senescence in salivary glands

Xiaohong Peng[1,2], Lara Barazzuol[1,2], Kärt Varendi[3], Jaan-Olle Andressoo[3,4], Rob P. Coppes[1,2]

[1]Department of Biomedical Sciences of Cells & Systems, [2]Department of Radiation Oncology, University Medical Center Groningen, University of Groningen, The Netherlands. [3]Institute of Biotechnology, University of Helsinki, Finland. [4]Institute of Biosciences and Medical Technology-BioMediTech, University of Tampere, Finland.

Manuscript in preparation

Abstract

Secretory function restoration is a challenge for regenerative therapy of radiation damaged salivary glands. Exogenously applied GDNF has been shown to improve post-irradiation secretory function potentially by enhancing proliferation of surviving salivary gland stem/progenitor cells (SGSCs). However, endogenous GDNF was shown to be highly upregulated in the ductal compartment of irradiated glands that exhibited severe morphological damage and impaired salivary secretion, the role of endogenous GDNF on SGSC survival and proliferation after irradiation remains unknown. Recently, GDNF has been shown to be highly expressed after irradiation acting as a core transcriptome signature of radiation-induced senescence in several cell lines. Cellular senescence is an irreversible state of cell cycle arrest induced by various stress factors and characterized by a distinct senescence-associated secretory phenotype (SASP). Here, by using the $GDNF^{Cre\text{-}ERT2}$-tdtomato mouse model, we demonstrate that GDNF dynamically changes during the cell cycle in proliferating SGSCs. However, upon radiation-induced cell cycle arrest, GDNF expression is highly upregulated together with senescence markers SA-β-gal and p16, and accumulates in enlarged lysosomes. Our data suggest that radiation-induced upregulation and accumulation of GDNF can act as a senescence marker. Therapies that activate the lysosomal degradation pathway might retard radiation-induced senescence and enhance SGSC regenerative potential .

Introduction

Xerostomia is a condition that may result from hyposalivation as a consequence of damage to the salivary glands by radiotherapy for head and neck cancer treatment, which may severely impair the patient's quality of life [1-3]. Current therapeutic options for xerostomia are limited and often result in temporary symptom improvement [4]. Stimulation of regeneration after irradiation using stem cell transplantation [5] or growth factors, such as keratinocyte growth factor (KGF) [6] and granulocyte-colony stimulating factor (G-CSF) [7], have demonstrated the potential of a stable improvement in salivary gland function.

Another interesting protein is glial cell line-derived neurotrophic factor (GDNF). GDNF is known to play an important role in the survival, function and growth of neurons [8,9] and to participate in renal morphogenesis [10] and spermatogenesis [11] by promoting stem cell self-renewal and proliferation. Interestingly, exogenous applied GDNF has been shown to improve post-irradiation secretory function potentially by enhancing proliferation of surviving salivary gland stem/progenitor cells (SGSCs) [12,13]. However, endogenous GDNF was shown to be highly upregulated in the ductal compartment of irradiated glands that exhibited severe morphological damage and impaired salivary secretion, while it was downregulated in glands treated with stem cell therapy [13] with improved morphology and secretory function [14]. Recently, GDNF has been shown to be highly expressed after irradiation acting as a core transcriptome signature of radiation-induced senescence in fibroblasts, keratinocytes and melanocytes [15]. Collectively, these studies raise the question of what is the role of GDNF in radiation-induced senescence in salivary glands.

Cellular senescence is an irreversible state of cell cycle arrest induced by various stress stimuli, such as radiation, cytotoxic drugs, oncogenes or telomere erosion [16-18]. Senescent cells are characterized by a distinct senescence-associated secretory phenotype (SASP), which includes cytokines, chemokines, extracellular

matrix proteases and growth factors [19,20]. Moreover, cellular senescence has been found to drive age-related tissue deterioration contributing to several diseases including neurodegenerative diseases [21,22], atherosclerosis [23] and osteoarthritis [24]. Interestingly, radiation has been shown to cause accumulation of senescent cells [25] contributing to the lack of regenerative response in salivary glands post-irradiation [26]. Notably, after irradiation, senescence markers, such as SA-β-galactosidase and p21, largely accumulate in the ductal cell compartment of the salivary glands, where the stem and progenitor cells have been suggested to be localized [26,27] (and Chapter 3 of this thesis). In this study, we aim to investigate the relation between GDNF expression and radiation-induced senescence.

Using SGSCs isolated from GDNF$^{Cre\text{-}ERT2}$-tdTomato reporter mice and cultured in 2D and 3D as organoids, the expression pattern of GDNF in proliferating untreated cells and cells after irradiation revealed that GDNF expression dynamically changes during the cell cycle. GDNF colocalizes with senescence markers in salivary gland tissue and 2D cultured cells, and increases and accumulates in lysosomes in cell cycle-arrested cells after irradiation. Collectively, these data suggest that GDNF could act as a novel additional marker of radiation-induced senescence in salivary glands.

Results

GDNF increased and colocalized with senescence after irradiation in salivary gland

We first investigated the expression of GDNF in combination with senescence in mouse salivary glands irradiated with 15 Gy. This radiation dose has previously been shown to largely eliminate the acinar cell compartment causing profound hyposalivation [14]. In accordance with other studies [12,13], murine salivary glands show high levels of GDNF at 8 weeks post-irradiation (IR) with 15 Gy compared to unirradiated control glands (Fig. 1a). This was further confirmed using qRT-PCR gene expression analysis (Fig. 1b). To further assess the role of

GDNF in radiation-induced senescence, irradiated salivary glands were co-stained for GDNF and SA-β-gal, a known marker of senescence [28]. Indeed GDNF (brown) largely colocalized with SA-β-gal (blue) in the ductal compartment of the salivary glands (Fig. 1c) where the stem/progenitor cells have been suggested to reside [27], whereas GDNF but not SA-β-gal expression was observed in control glands. These data suggest that GDNF may play a role in radiation-induced cellular senescence in the salivary gland.

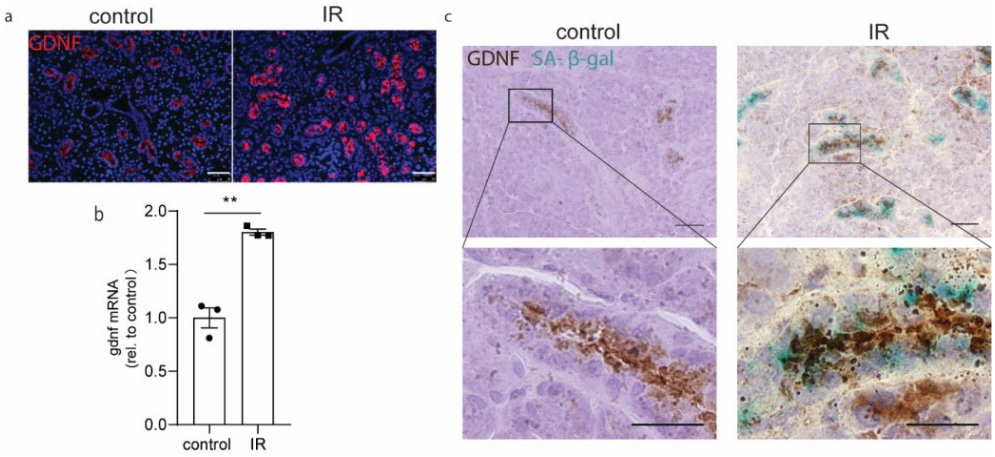

Fig.1 GDNF co-localizes with SA-β-gal in irradiated salivary gland tissue. 6-8 week-old C57BL/6 mice were locally irradiated with 15 Gy to the salivary glands. Salivary glands were collected 8 weeks post-irradiation (IR) for analysis. **a)** GDNF immunofluorescence staining of mouse salivary gland paraffin sections (control vs IR). Scale bar=50μm. **b)** qRT-PCR analysis of the expression of Gdnf in salivary glands 8 weeks post-IR. **c)** SA-β-gal and GDNF immunohistochemistry staining of mouse salivary gland frozen sections (control vs IR). Data represent mean ± SEM. Student t-test, **p <0.01. Pictures are representatives of 3 independent experiments.

To further investigate the role of GDNF in radiation-induced cellular senescence, mouse SGSCs derived organoids [14] were used to assess stem cell potential. 5 day old (D5) organoids were irradiated with 7 Gy, a dose known to induce senescence [29,30] (and Chapter 3), and were analyzed 7 days later (D12) allowing the formation of senescent cells (Fig. 2a). As control, D5 organoids were used. GDNF

expression was significantly increased in salivary gland organoids after irradiation when compared to control. The highest GDNF expression was observed in the middle of the irradiated organoids, where also the most intense staining of SA-β-gal was observed (Fig. 2b-c). To better understand the role of GDNF in radiation-induced senescent cells, single cells derived from organoids were reseeded in 2D (Fig. 2d), improving visualization, and cultured for 2 days to reach 80-90% confluence. The cells were irradiated with 7 Gy and analyzed 7 days later (D9) allowing the formation of senescent cells (Fig. 2d). Interestingly, GDNF was highly expressed in control cells that had just underwent cell division but were lacking SA-β-gal activity (Fig. 2e, left panel). After irradiation, the cells were enlarged with an irregular shape and showed substantially increased SA-β-gal activity indicating that the cells were senescent (Fig. 2e, right panel, Supplementary Fig. 1a). Interestingly, most cells appeared to be positive for GDNF. In addition, after irradiation, GDNF was highly expressed and co-localized with the senescence marker P16(INK4a) (Fig. 2f) [31]. However, control cells expressed only GDNF (Fig. 2f).

It has been reported that GDNF is targeted to lysosomes for degradation [32]. To further substantiate if GDNF is degraded properly in radiation-induced senescent cells, expression of GDNF and the lysosomal marker LAMP1 was investigated. Staining for the lysosomal membrane protein LAMP-1 showed that irradiated cells had enlarged lysosomes compare to unirradiated cells (Fig. 2g, Supplementary Fig. 1b). GDNF was highly upregulated and accumulated post-irradiation close or within LAMP-1 positive lysosomes (Fig. 2g), suggesting that GDNF may not be degraded properly or is upregulated in irradiated senescent cells (Supplementary Fig. 2b). This is consistent with the observation that lysosomal content is increased in senescent cells [33].

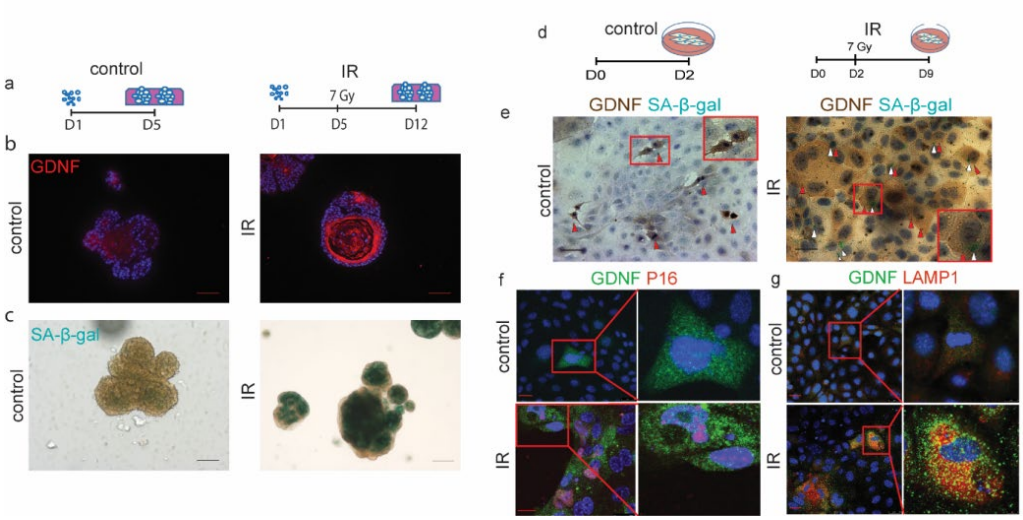

Fig. 2 GDNF expression after irradiation in salivary gland cells cultured in 2D and in 3D as organoids. a) Experimental design for (b-c). **b)** GDNF immunofluorescence (IF) staining (red) and **c)** SA-β-gal staining (blue) was performed on whole mount organoids collected at the indicated time points in control and irradiated (IR) organoids. Scale bar=50 µm. **d)** Experimental design for (e-g). **e)** SA-β-gal staining (blue) co-stained with GDNF (brown) on 2D cultured salivary gland cells. Scale bar=50 µm. **f-g)** Representative IF images of GDNF (green) co-staining with P16 (red) (**f**) and LAMP1 (red) (**g**) on 2D cultured salivary gland cells at the indicated time points in control and IR cells. Scale bar=25 µm.

GDNF expression dynamically changes during cell cycle

Interestingly, most of the GDNF positive cells in the unirradiated situation were cells undergoing or that have just completed cell division (Fig. 2e, left panel). To verify this, we next looked at GDNF expression using GDNF$^{Cre\text{-}ERT2}$-tdTomato transgenic mice. In this mouse model upon tamoxifen treatment GDNF-expressing cells are genetically labeled by persisting tdTomato expression from the constitutively expressed Rosa 26 locus (Fig. 3a). Indeed upon tamoxifen treatment (induction efficiency of 16.4±1.4%) tdTomato/GDNF expressing cells (Fig. 3a-c) exhibited, a high tdTomato positive organoid formation ability (80±2.83%, percentage of tdTomato positive organoids) (Supplementary Fig. 2a-c) indicative

of GDNF related stemness. Similar results were obtained when tamoxifen was administered to more maturated budding organoids (Supplementary Fig. 2d-e) which induced tdTomato expression in some cells of the organoids 24 h later. These data confirm that GDNF is expressed at different stages of organoid development. Interestingly, salivary gland stem cell selfrenewal assay showed no significance difference between $GDNF^{cko/ko}$ (het) and $GDNF^{ko/ko}$(ko) mice (Supplementary Fig. 3a-b), while lack of GDNF leads to promotion of SGSC maturation as quantified by the change in organoid morphology (budding) (Supplementary Fig. 3c-d), indicating that the role of GDNF can vary with its level. GDNF may promote SGSC self-renewal by inhibiting SGSC differentiation.

To further elucidate the GDNF expression pattern during cell cycle at a single cell level, we analyzed cells dissociated from organoids, cultured in 2D and treated with tamoxifen (Fig. 3b). Indeed 24 h after tamoxifen treatment, tdTomato was expressed in cells undergoing or that have just finished cell division (Fig. 3c, supplementary Fig. 2f), confirming our findings using the GDNF antibody-based staining (Fig. 3d, supplementary Fig. 2g). Interestingly, GDNF expression as detected by antibody colocalized with tdTomato in proliferating cells (arrow head) and disappeared in those cells that had completed cell division (arrow), indicating that GDNF expression may dynamically change during cell cycle (Fig. 3e).

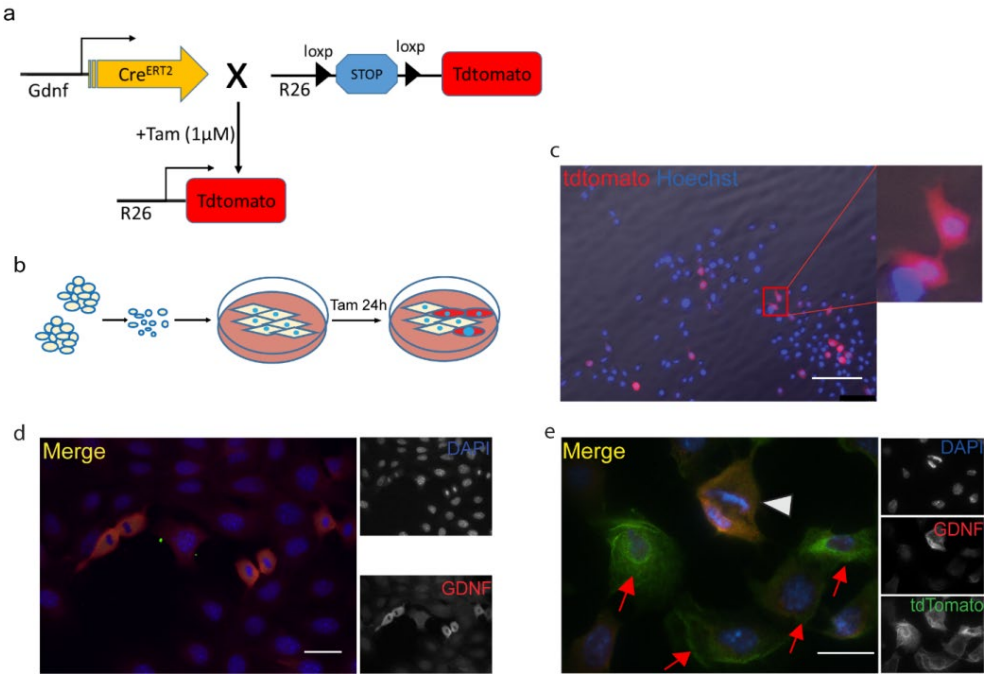

Fig. 3 GDNF expression during salivary gland cell proliferation. a) Schematic representation of the GDNF$^{Cre\text{-}ERT2}$-tdTomato transgene. GDNF$^{Cre\text{-}ERT2}$ mice were crossed with R26-tdTomato mice to generate GDNF$^{Cre\text{-}ERT2}$-tdTomato mice. Salivary glands cells were cultured and recombination was induced by 1 µM tamoxifen (Tam). **b)** Schematic overview of the study design for experiments carried out in ***c-e***. Organoids derived from salivary gland cells of GDNF$^{Cre\text{-}ERT2}$-tdTomato mice were disrupted into single cells and reseeded into 2D. When 70% confluence was reached the cells were treated with 1 µM Tam for 24 h. **c)** Representative live images of 2D SG cells of GDNF$^{Cre\text{-}ERT2}$-tdtomato mice after 24 h Tam treatment. Hoechst 33342 was used to visualize nuclei. Scale bar=100 µm. tdTomato positive cells were quantified after 24 h of Tamoxifen, 16.4±1.4% cells were induced. Data represent mean ± SEM. **d)** GDNF immunofluorescence staining of 2D cultured SG cells from GDNF$^{Cre\text{-}ERT2}$-tdtomato mice. Scale bar=25 µm. **e)** GDNF and tdTomato IF staining of 2D SG cells from GDNF$^{Cre\text{-}ERT2}$-tdtomato mice. Scale bar=25 µm. Pictures are representatives of 3 independent experiments.

GDNF expression in radiation-induced senescent cells

Senescence is known as a state of irreversible cell cycle arrest, which can be induced by radiation. To further elucidate the role of GDNF in radiation-induced cell cycle arrest, we used our previously developed senescent organoid model. D5 organoids were irradiated with 7 Gy and analyzed 7 days later, a dose and a time known to induce senescence *in vitro* [29,30] (see Chapter 3). As controls, D5 and age-matched D12 organoids were used (Fig. 4a). Considerable G0/G1 cell cycle growth arrest (81.43±0.48%; $p<0.001$ compared to D5 control) and decreased S-phase cell population (2.57±0.31%, $p<0.01$ compared to D5 control) were observed in D12 control organoids, suggesting cell cycle exit and decreased proliferation, potentially due to quiescence, senescence or cell differentiation overtime in culture. Whereas irradiated organoids showed an increase in G2/M (24.1±2%) and a decrease in the S phase cell population (3.36± 0.24%, $P<0.01$) (Fig. 4b, supplementary Fig. 4a) compared to D5 control organoids. This is in line with previous data that irradiation activates cell cycle checkpoints arresting the cell cycle at the G1/S and G2/M phases [34]. An increased proportion of multinucleated cells (8.9±1.9%, $p<0.05$ compared to D5 control), a characteristic morphological change of senescence [18], was also observed in irradiated organoids.

GDNF and PI flow cytometry analysis of cells dissociated from control D5, D12, and irradiated organoids (supplementary Fig. 4b-4c) revealed that 96.9±0.95% of the proliferating cells were GDNF positive (Fig. 4c, D5) in D5 control cells. This proportion decreased in D12 control cells (58.4±6.55%, $p<0.01$ compared to D5 control) (Fig. 4c, D12), in which only 48.9% of cells in G1 phase were GDNF positive ($P<0.0001$ compared to D5) (Fig. 4d, D12 organoids). Compared to the D5 control group, irradiated organoids show a slight decrease in the total number of GDNF positive cells (88.9±1.1%, $P<0.01$) (Fig. 4c, IR). Among the irradiated cells in G1 phase 85.2% were GDNF positive (Fig. 4d, IR). Strikingly, almost all the G2/M and multinucleated cells were GDNF positive (Fig. 4d), which was

confirmed by the IF staining pattern of GDNF in 2D cultured cells (Fig. 4e). Interestingly, D12 control organoids show the lowest level of GDNF expression (Fig. 4d-4e) while the highest amount of cells in G0/G1 phase (Fig. 4b), indicating that most of the cells might be in the G0 phase rather than the G1 phase, as has been suggested to occur after senescence [35]. Moreover, irradiated 2D cultured organoid derived cells showed morphological changes, larger size and multinucleated, compared to cells derived from D5 and D12 control organoids (Fig. 4e). This is in line with Fig. 2 showing that a proportion of the irradiated cells undergo senescence.

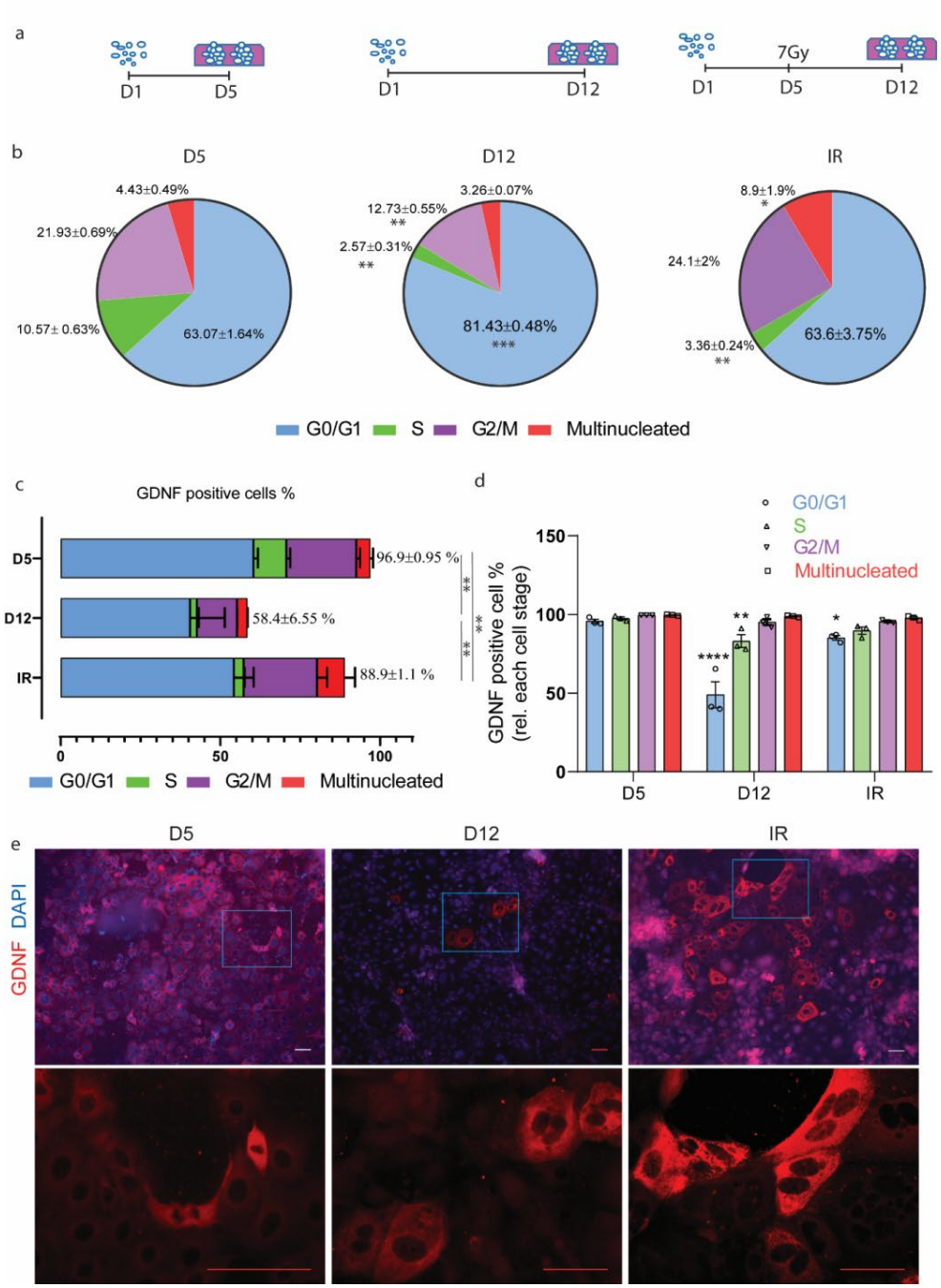
a
D1
D5
D1
D12
7Gy
D1
D5
D12
b
D5
4.43±0.49%
21.93±0.69%
10.57± 0.63%
63.07±1.64%
D12
3.26±0.07%
12.73±0.55%
**
2.57±0.31%
**
81.43±0.48%
***
IR
8.9±1.9%
*
24.1±2%
3.36±0.24%
**
63.6±3.75%
G0/G1
S
G2/M
Multinucleated
c
GDNF positive cells %
D5
D12
IR
96.9±0.95 %
58.4±6.55 %
88.9±1.1 %
0
50
100
G0/G1
S
G2/M
Multinucleated
d
G0/G1
S
G2/M
Multinucleated
GDNF positive cell %
(rel. each cell stage)
150
100
50
0
D5
D12
IR
e
D5
D12
IR
GDNF
DAPI

Fig. 4 GDNF expression analysis after irradiation. a) Schematic overview of the study design for experiments carried out in panels **b-d**. Mouse salivary gland organoids were cultured and irradiated with 7 Gy photons (IR) at day 5 in culture (D5) and collected 7 days later (D12). 5-day-old (D5) and age-matched 12-day-old (D12) organoids were used as controls. **b)** Pie charts showing cell cycle distribution of cells dissociated from D5, D12 and IR organoids, determined using flow cytometry. **c)** GDNF positive cells distribution in different cell cycle phases of cells dissociated from D5, D12 and IR organoids, determined using flow cytometry. **d)** GDNF positive cells percentage normalized to each cell cycle phase in D5, D12 and IR organoids, determined using flow cytometry. **e)** GDNF IF staining of 2D cultured SG cells dissociated from D5, D12 and IR organoids. Scale bar=50 μm. Data were compared to D5 control, Data represent mean ± SEM. N=3 mice. Student t-test (c) and two-way Anova (b,d), *p<0.05, **p<0.01, ***p<0.001, ****p<0.0001.

Discussion

Despite multiple studies have been done, the function of endogenous GDNF remains poorly understood. Here, by using the $GDNF^{Cre\text{-}ERT2}$-tdtomato mouse model, we demonstrate that GDNF dynamically changes during the cell cycle in proliferating SGSCs. However, upon radiation-induced cell cycle arrest, GDNF expression is upregulated together with senescence markers SA-β-gal and p16, and accumulates in enlarged lysosomes.

GDNF is known to play an important role in neuronal survival, renal morphogenesis and spermatogenesis by promoting stem cell self-renewal and proliferation [11,36-38]. Recently, it has been reported that GDNF also promotes salivary gland stem cell self-renewal capacity [12,13]. Interestingly, $GDNF^{ko/ko}$ mice derived salivary gland organoid cultures showed no change in SGSC self-renewal capacity, however, enhanced SGSC maturation was observed, suggesting that higher levels of GDNF may drive SGSC self-renewal and proliferation by inhibiting cell differentiation. A similar phenomenon was also observed in spermatogonial stem cells in which the role of GDNF varies with its expression level. The spermatogonial stem cells undergo differentiation with low level of

GDNF, while they undergo self-renewal with high level of GDNF [11]. However, since $GDNF^{ko/ko}$ mice do not survive after birth due to the lack of the entire enteric nervous system and kidney agenesis [10], the exact role of GDNF on adult SGSC self-renewal and differentiation remains to be elucidated.

Previous data showed that GDNF was highly expressed and localized in the secretory ducts of irradiated murine and human salivary glands [12,13], where most senescence was shown to occur [26]. These findings raise the possibility that GDNF may play a role in radiation-induced senescence. Indeed, RNA sequencing and qPCR data showed that GDNF expression is consistently increased in radiation-induced senescence in several cell lines, including fibroblasts, keratinocytes and melanocytes [15]. One possible mechanism by which GDNF may contribute to radiation-induced senescence is by activating the NF-κB signaling pathway, which is a major inducer of cellular senescence and SASP [39,40]. Indeed, it has been shown that the noncanonical pathway of NF-κB p62/p52 signaling [41,42] was activated by GDNF and was involved in the antiapoptotic role of GDNF via upregulation of the antiapoptotic proteins Bcl2 and Bcl-w [39,43,44]. Interestingly, our data showed that GDNF was upregulated and accumulated in enlarged lysosomes together with the expression of senescence markers, SA-β-gal and p16, in irradiated salivary gland organoid-derived cells cultured in 2D. This finding seems to resemble the condition of senescence caused by radiation where the cell cycle is blocked while growth is stimulated leading to cellular hypertrophy and subsequent compensatory responses, such as SA-β-gal positivity and lysosomal activation [35,45]. In addition, it has been reported that GDNF is targeted to lysosomes for degradation [32]. Based on our own finding that GDNF dynamically changes during the cell cycle while it accumulates in enlarged lysosomes during radiation-induced cell cycle arrest, we speculate that GDNF is not properly degraded after irradiation due to the dysfunction of lysosomes, which may be due to autophagy impairment [46]. Activation of the lysosomal pathway by restoring autophagy might be a way to reduce senescence and enhance SGSC

regenerative potential. However, whether GDNF functions as a regenerative factor or a senescence enhancer may depend on issues such as timing, inducer and expression levels. Therefore, inhibition/stimulation of GDNF specifically in SGSC derived organoids may represent a way to further elucidate its function during the cell cycle and radiation-induced senescence.

Our study indicates that GDNF expression can be used to confirm cellular senescence together with other senescence markers. However, whether GDNF acts as a cause or a consequence of senescence remains to be further investigated.

Materials and Methods

Mice

8 to 12-week-old female C57BL/6 mice (Envigo, Harlan, The Netherlands) were bred in the Central Animal Facility of University Medical Center, Groningen. $GDNF^{Cre\text{-}ERT2}$-tdTomato transgenic mice, $GDNF^{cKO/KO}$ and $GDNF^{KO/KO}$ mice were bred in the Central Animal Facility at the Institute of Biotechnology, University of Helsinki, Finland. The mice were maintained under conventional feeding conditions and water. All experiments were approved by the Ethical Committee of the University of Groningen.

Isolation of salivary gland cells and organoid culture

Murine submandibular salivary glands were dissected from 8-12 week-old female p16-3MR mice. Animal experimental procedures were approved by the Central Committee Animal Experimentation of the Dutch government and the Institute Animal Welfare Body at the University Medical Centre Groningen. Salivary gland cells were isolated and cultured to form organoids as described previously [3,14,47]. In short, salivary glands were mechanically and enzymatically dissociated and cultured in DMEM-12 (Gibco/Invitrogen, 11320-074) medium consisting of 1% penicillin/streptomycin (Gibco), glutamax (2 mM; ThermoFischer

Scientific, 35050038), EGF (20 ng/ml; Sigma-Aldrich, E9644), FGF2 (20 ng/ml; peprotech, 100-18B), N2 (1×; Gibco, 17502-048), insulin (10 μg/ml; Sigma-Aldrich, I6634), and dexamethasone (1 μM; Sigma-Aldrich, d4902), here called minimal medium. After three days, primary spheres were dissociated into single cells, seeded in Matrigel and cultured in minimal medium supplemented with Y-27632 (10 μM; Abcam, ab120129), 10% R-spondin1 conditioned medium (provided by C. Kuo), and 50% Wnt3a conditioned medium to form organoids. After 7 days organoids were passaged by dissociation into single cells and cultured as described above.

Organoid Differentiation

Primary salispheres (passage 0,Day 5 old in MM medium) were mixed properly with differentiation matrix ingredients (40% collagen and 60% growth factor reduced matrigel (BD Biosciences) and seeded 100 μl per well in 96 wells plates. After incubate at 37℃ for 20 minutes, 150 μl differentiation medium containing fetal calf serum (FCS, Invitrogen), Hepatocyte growth factor (HGF) and DAPT was added and changed every 4 days. Differentiated budding structures were checked 6 days later.

Radiation treatment on salivary gland cells and organoids

Photon irradiation were performed using a Cesium-137 source with a dose rate of 0.59 Gy/min. Senescence induction experiments were performed with 7 Gy on 5-day-old (D5) organoids cultured in Matrigel in 12-well plates, or on 70% confluent 2D cultured salivary gland cells dissociated from the organoids.

SA-β-galactosidase staining

Organoids/cells were collected 7 days after (sham) irradiation, fixed and stained overnight with X-Gal solution according to the manufacturer's instructions (Merck

Millipore, KAA002RF). Senescent cells were identified as blue-stained cells under light microscopy.

qRT-PCR

Cells were collected at designated time points. Total cellular RNA was extracted following the manufacturer's instructions (Qiagen, RNeasy Mini Kit, Ref 74104) to measure expression of cell cycle genes Cdkn2a ($p16^{Ink4a}$), Cdkn1a (p21) and SASP genes (including Il6, Mcp1 Cxcl1), and the senescence transcriptome core signature Gdnf in mouse salivary gland stem/progenitor cells and salivary glands tissue, respectively. The primer sequences are listed in Supplementary Table 1. RNA reverse transcription was performed as described previously [13]. First-strand cDNA synthesis was performed by using 500 ng total RNA, 1 µl dNTP Mix(10 mM), 1 µl random primers (100 ng), 4 µl 5x First-stand Buffer, 2 µl DTT(0.1 M), 1 µl RNase OUTTM (40 units/µl), and 1 µl M-MLV RT (200 units), 20 µl in total for each reaction volume. To measure gene expression, the SYBR assay kit (Bio-Rad) was used. Briefly, 2.5 µl cDNA was mixed with 6.25 µl SYBR Green PCR Master Mix and 3.75 µl primers mix (20 µl forward primer, 20 µl reverse primer and 1160 µl dH2O) for genes of interest. qPCR conditions were as follow: 95℃ for 3 min, 39 x (95℃ for 10 s, 55℃ for 10 s and 72℃ for 30 s), 95℃ for 10 s, 65℃ for 5 s, 95℃ for 50 s. All reactions were run in triplicate on a BIO-RAD Real-Time PCR System. All reagents mentioned above are from Invitrogen.

Immunostaining

Mouse salivary gland tissues were fixed with 4% formaldehyde (24 h at room temperature) and processed for paraffin embedding. Following dehydration, the tissue was embedded in paraffin and sliced into 5-µm sections. The sections were dewaxed, boiled for 8 min in pre-heated 10 mM citric acid retrieval buffer (pH 6.0) containing 0.05% Tween 20; 2D cultured salivary gland cells were fixed with 4% Paraformaldehyde for 10min and incubate with 0.1% triton for 5min, washed

thoroughly prior to primary antibody exposure, and labeled for the following markers: GDNF (Abcam, ab18956); P16, Abcam, ab54210); LAMP1 (Abcam, ab25245), tdTomato (Anti RFP antibody, Biovision3984-100). For immunofluorescence staining, Alexa Fluor 488 donkey anti-rabbit (Life Technologies, A-21206) or Alexa Fluor 594 goat anti-rabbit (Thermofischer a11012), Alexa Fluor 594 donkey anti-mouse (Life Technologies, A21203) or Alexa Fluor 594 donkey anti-rat (Thermofischer a21209), conjugates at 1:400 dilution were used as secondary antibodies. Nuclear staining was performed with DAPI (Sigma-Aldrich). For immunohistochemistry (IHC) staining, specific secondary biotin-carrying antibodies (Dako), an avidin-biotin-horseradish peroxidase complex (ELITE ABC Kit, Vector Laboratories) and the diaminobenzidine chromogen were accomplished according to standard IHC protocol. Nuclear staining was performed with hematoxylin. For SA-β-galactosidase and IHC double staining, SA-β-gal staining was performed first followed by IHC staining.

Tamoxifen-induced gene recombination

Single cells or salivary gland organoids derived from $GDNF^{Cre\text{-}ERT2}$-tdTomato transgenic mice were induced by 1 μM tamoxifen for 24h, nuclear counterstaining was performed with Hoechst 33258 (Sigma-Aldrich) for 10 min at room temperature.

Flow cytometry

Salivary gland organoids were harvested at designated time points. After two washes with PBS, cells were fixed with 70% ethanol, incubated overnight at 4℃. Cells were collected by spin down 5 min at 1000 rpm at 4℃. Cells were incubated with anti-GDNF antibody (Abcam, ab18956) in PBS. 1% BSA (bovine serum albumin) (1:50) at room temperature for 2 hours, followed by washing with PBS, then incubated with Alexa 488 goat anti-Rabbit secondary antibody (a11008)(1:50)

at room temperature for 30 mins in the dark, followed by washing with PBS. After two washes with PBS, cells were treated with 20 µl DNase free RNase A to remove residual RNA (Sigma Aldrich) and incubated for 30 mins at 37℃. 400 µl of Propidium Iodide solution was added to cells and incubated for 1 h at room temperature. Samples were analyzed by using the XDP flow cytometry machine. The Flowjo software was used to determine the distribution of GDNF positive and negative cells in the G0/G1, S and G2/M phases.

Statistical analysis

Statistical comparisons using the student t test as indicated were performed using GraphPad Prism 8.0 software. Numbers (n) for tested groups are stated in the figure legends. All values are represented as mean ± SEM, $P<0.05$ considered as statistically significant.

References

[1] Vissink A, Burlage FR, Spijkervet FK, Jansma J, Coppes RP. Prevention and treatment of the consequences of head and neck radiotherapy. Crit Rev Oral Biol Med 2003;14:213-225.

[2] Swick A, Kimple RJ. Wetting the whistle: neurotropic factor improves salivary function. J Clin Invest 2014;124:3282-3284.

[3] Nagle PW, Hosper NA, Ploeg EM, van Goethem MJ, Brandenburg S, Langendijk JA et al. The In Vitro Response of Tissue Stem Cells to Irradiation With Different Linear Energy Transfers. Int J Radiat Oncol Biol Phys 2016;95:103-111.

[4] Sagowski C, Wenzel S, Metternich FU, Kehrl W. Studies on the radioprotective potency of amifostine on salivary glands of rats during fractionated irradiation: acute and late effects. Eur Arch Otorhinolaryngol 2003;260:42-47.

[5] Pringle S, Maimets M, van der Zwaag M, Stokman MA, van Gosliga D, Zwart E et al. Human Salivary Gland Stem Cells Functionally Restore Radiation Damaged Salivary Glands. Stem Cells 2016;34:640-652.

[6] Lombaert IM, Brunsting JF, Wierenga PK, Kampinga HH, de Haan G, Coppes RP. Keratinocyte growth factor prevents radiation damage to salivary glands by expansion of the stem/progenitor pool. Stem Cells 2008;26:2595-2601.

[7] Lombaert IM, Wierenga PK, Kok T, Kampinga HH, deHaan G, Coppes RP. Mobilization of bone marrow stem cells by granulocyte colony-stimulating factor ameliorates radiation-induced damage to salivary glands. Clin Cancer Res 2006;12:1804-1812.

[8] Lin LF, Doherty DH, Lile JD, Bektesh S, Collins F. GDNF: a glial cell line-derived neurotrophic factor for midbrain dopaminergic neurons. Science 1993;260:1130-1132.

[9] Hoffer BJ, Hoffman A, Bowenkamp K, Huettl P, Hudson J, Martin D et al. Glial cell line-derived neurotrophic factor reverses toxin-induced injury to midbrain dopaminergic neurons in vivo. Neurosci Lett 1994;182:107-111.

[10] Sainio K, Suvanto P, Davies J, Wartiovaara J, Wartiovaara K, Saarma M et al. Glial-cell-line-derived neurotrophic factor is required for bud initiation from ureteric epithelium. Development 1997;124:4077-4087.

[11] Meng X, Lindahl M, Hyvonen ME, Parvinen M, de Rooij DG, Hess MW et al. Regulation of cell fate decision of undifferentiated spermatogonia by GDNF. Science 2000;287:1489-1493.

[12] Xiao N, Lin Y, Cao H, Sirjani D, Giaccia AJ, Koong AC et al. Neurotrophic factor GDNF promotes survival of salivary stem cells. J Clin Invest 2014;124:3364-3377.

[13] Peng X, Varendi K, Maimets M, Andressoo JO, Coppes RP. Role of glial-cell-derived neurotrophic factor in salivary gland stem cell response to irradiation. Radiother Oncol 2017;124:448-454.

[14] Maimets M, Rocchi C, Bron R, Pringle S, Kuipers J, Giepmans BN et al. Long-Term In Vitro Expansion of Salivary Gland Stem Cells Driven by Wnt Signals. Stem Cell Reports 2016;6:150-162.

[15] Hernandez-Segura A, de Jong TV, Melov S, Guryev V, Campisi J, Demaria M. Unmasking Transcriptional Heterogeneity in Senescent Cells. Curr Biol 2017;27:2652-2660.e4.

[16] Childs BG, Durik M, Baker DJ, van Deursen JM. Cellular senescence in aging and age-related disease: from mechanisms to therapy. Nat Med 2015;21:1424-1435.

[17] Munoz-Espin D, Rovira M, Galiana I, Gimenez C, Lozano-Torres B, Paez-Ribes M et al. A versatile drug delivery system targeting senescent cells. EMBO Mol Med 2018;10:10.15252/emmm.201809355.

[18] Kuilman T, Michaloglou C, Mooi WJ, Peeper DS. The essence of senescence. Genes Dev 2010;24:2463-2479.

[19] Coppe JP, Desprez PY, Krtolica A, Campisi J. The senescence-associated secretory phenotype: the dark side of tumor suppression. Annu Rev Pathol 2010;5:99-118.

[20] Campisi J, d'Adda di Fagagna F. Cellular senescence: when bad things happen to good cells. Nat Rev Mol Cell Biol 2007;8:729-740.

[21] Tan FC, Hutchison ER, Eitan E, Mattson MP. Are there roles for brain cell senescence in aging and neurodegenerative disorders? Biogerontology 2014;15:643-660.

[22] Luo XG, Ding JQ, Chen SD. Microglia in the aging brain: relevance to neurodegeneration. Mol Neurodegener 2010;5:12-1326-5-12.

[23] Childs BG, Baker DJ, Wijshake T, Conover CA, Campisi J, van Deursen JM. Senescent intimal foam cells are deleterious at all stages of atherosclerosis. Science 2016;354:472-477.

[24] Jeon OH, Kim C, Laberge RM, Demaria M, Rathod S, Vasserot AP et al. Local clearance of senescent cells attenuates the development of post-traumatic osteoarthritis and creates a pro-regenerative environment. Nat Med 2017;23:775-781.

[25] Le ON, Rodier F, Fontaine F, Coppe JP, Campisi J, DeGregori J et al. Ionizing radiation-induced long-term expression of senescence markers in mice is independent of p53 and immune status. Aging Cell 2010;9:398-409.

[26] Marmary Y, Adar R, Gaska S, Wygoda A, Maly A, Cohen J et al. Radiation-Induced Loss of Salivary Gland Function Is Driven by Cellular Senescence and Prevented by IL6 Modulation. Cancer Res 2016;76:1170-1180.

[27] Pringle S, Van Os R, Coppes RP. Concise review: Adult salivary gland stem cells and a potential therapy for xerostomia. Stem Cells 2013;31:613-619.

[28] Debacq-Chainiaux F, Erusalimsky JD, Campisi J, Toussaint O. Protocols to detect senescence-associated beta-galactosidase (SA-betagal) activity, a biomarker of senescent cells in culture and in vivo. Nat Protoc 2009;4:1798-1806.

[29] Demaria M, Ohtani N, Youssef SA, Rodier F, Toussaint W, Mitchell JR et al. An essential role for senescent cells in optimal wound healing through secretion of PDGF-AA. Dev Cell 2014;31:722-733.

[30] Kang C, Xu Q, Martin TD, Li MZ, Demaria M, Aron L et al. The DNA damage response induces inflammation and senescence by inhibiting autophagy of GATA4. Science 2015;349:aaa5612.

[31] Coppe JP, Rodier F, Patil CK, Freund A, Desprez PY, Campisi J. Tumor suppressor and aging biomarker p16(INK4a) induces cellular senescence without the associated inflammatory secretory phenotype. J Biol Chem 2011;286:36396-36403.

[32] Glerup S, Lume M, Olsen D, Nyengaard JR, Vaegter CB, Gustafsen C et al. SorLA controls neurotrophic activity by sorting of GDNF and its receptors GFRalpha1 and RET. Cell Rep 2013;3:186-199.

[33] Hernandez-Segura A, Nehme J, Demaria M. Hallmarks of Cellular Senescence. Trends Cell Biol 2018;28:436-453.

[34] Wang B. Analyzing cell cycle checkpoints in response to ionizing radiation in mammalian cells. Methods Mol Biol 2014;1170:313-320.

[35] Blagosklonny MV. Cell cycle arrest is not senescence. Aging (Albany NY) 2011;3:94-101.

[36] Sariola H, Saarma M. Novel functions and signalling pathways for GDNF. J Cell Sci 2003;116:3855-3862.

[37] Airaksinen MS, Saarma M. The GDNF family: signalling, biological functions and therapeutic value. Nat Rev Neurosci 2002;3:383-394.

[38] Lin LF, Doherty DH, Lile JD, Bektesh S, Collins F. GDNF: a glial cell line-derived neurotrophic factor for midbrain dopaminergic neurons. Science 1993;260:1130-1132.

[39] Sun Y, Huang X, Liu M, Cao J, Chen J, Wang H et al. A new alternative NF-kappaB pathway mediated the neuroprotection of GDNF on 6-OHDA-induced DA neurons neurotoxicity. Brain Res 2012;1437:38-49.

[40] Salminen A, Kauppinen A, Kaarniranta K. Emerging role of NF-kappaB signaling in the induction of senescence-associated secretory phenotype (SASP). Cell Signal 2012;24:835-845.

[41] Karin M, Yamamoto Y, Wang QM. The IKK NF-kappa B system: a treasure trove for drug development. Nat Rev Drug Discov 2004;3:17-26.

[42] Lich JD, Williams KL, Moore CB, Arthur JC, Davis BK, Taxman DJ et al. Monarch-1 suppresses non-canonical NF-kappaB activation and p52-dependent chemokine expression in monocytes. J Immunol 2007;178:1256-1260.

[43] Cao JP, Wang HJ, Yu JK, Liu HM, Gao DS. The involvement of NF-kappaB p65/p52 in the effects of GDNF on DA neurons in early PD rats. Brain Res Bull 2008;76:505-511.

[44] Cao JP, Niu HY, Wang HJ, Huang XG, Gao DS. NF-kappaB p65/p52 plays a role in GDNF up-regulating Bcl-2 and Bcl-w expression in 6-OHDA-induced apoptosis of MN9D cell. Int J Neurosci 2013;123:705-710.

[45] Sherr CJ, DePinho RA. Cellular senescence: mitotic clock or culture shock? Cell 2000;102:407-410.

[46] Tai H, Wang Z, Gong H, Han X, Zhou J, Wang X et al. Autophagy impairment with lysosomal and mitochondrial dysfunction is an important characteristic of oxidative stress-induced senescence. Autophagy 2017;13:99-113.

[47] Nanduri LS, Maimets M, Pringle SA, van der Zwaag M, van Os RP, Coppes RP. Regeneration of irradiated salivary glands with stem cell marker expressing cells. Radiother Oncol 2011;99:367-372.

[48] Kopra JJ, Panhelainen A, Af Bjerken S, Porokuokka LL, Varendi K, Olfat S et al. Dampened Amphetamine-Stimulated Behavior and Altered Dopamine Transporter Function in the Absence of Brain GDNF. J Neurosci 2017;37:1581-1590.

[49] Kumar A, Kopra J, Varendi K, Porokuokka LL, Panhelainen A, Kuure S et al. GDNF Overexpression from the Native Locus Reveals its Role in the Nigrostriatal Dopaminergic System Function. PLoS Genet 2015;11:e1005710.

Supplemental Figures

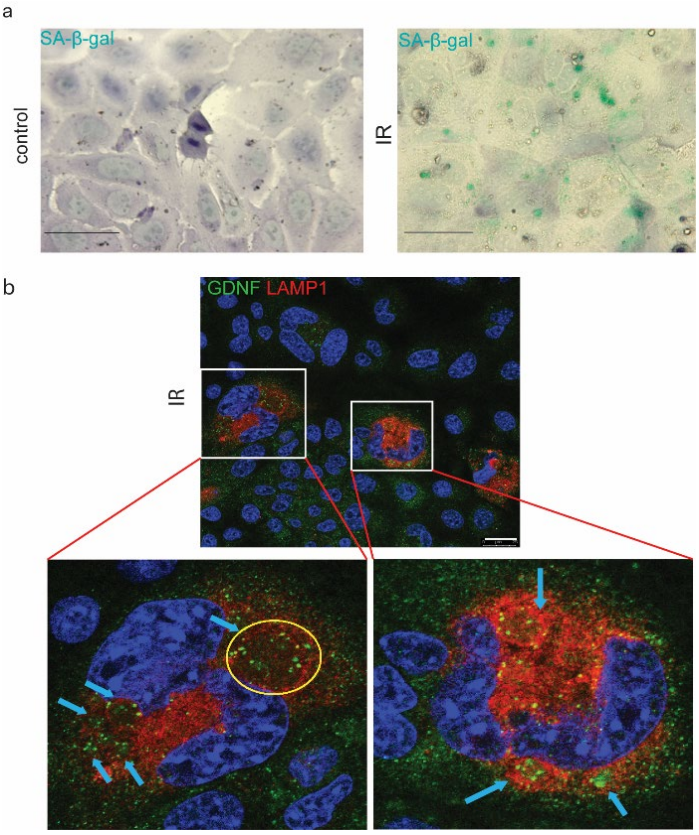

Supplementary Fig. 1 Expression of senescence, GDNF and lysosomal marker after irradiation in organoid-derived salivary gland cells cultured in 2D. a) SA-β-gal staining (blue) was performed on 2D cultured salivary gland cells collected at the indicated time points in control (day 2, D2) and 7 Gy IR (D9) groups. Scale bar=50 μm. **b)** Representative IF images of GDNF (green) and LAMP1 (red) co-staining on 2D cultured salivary gland cells 7 days after IR. Blue is DAPI. Arrows point out the enlarged lysosomes.

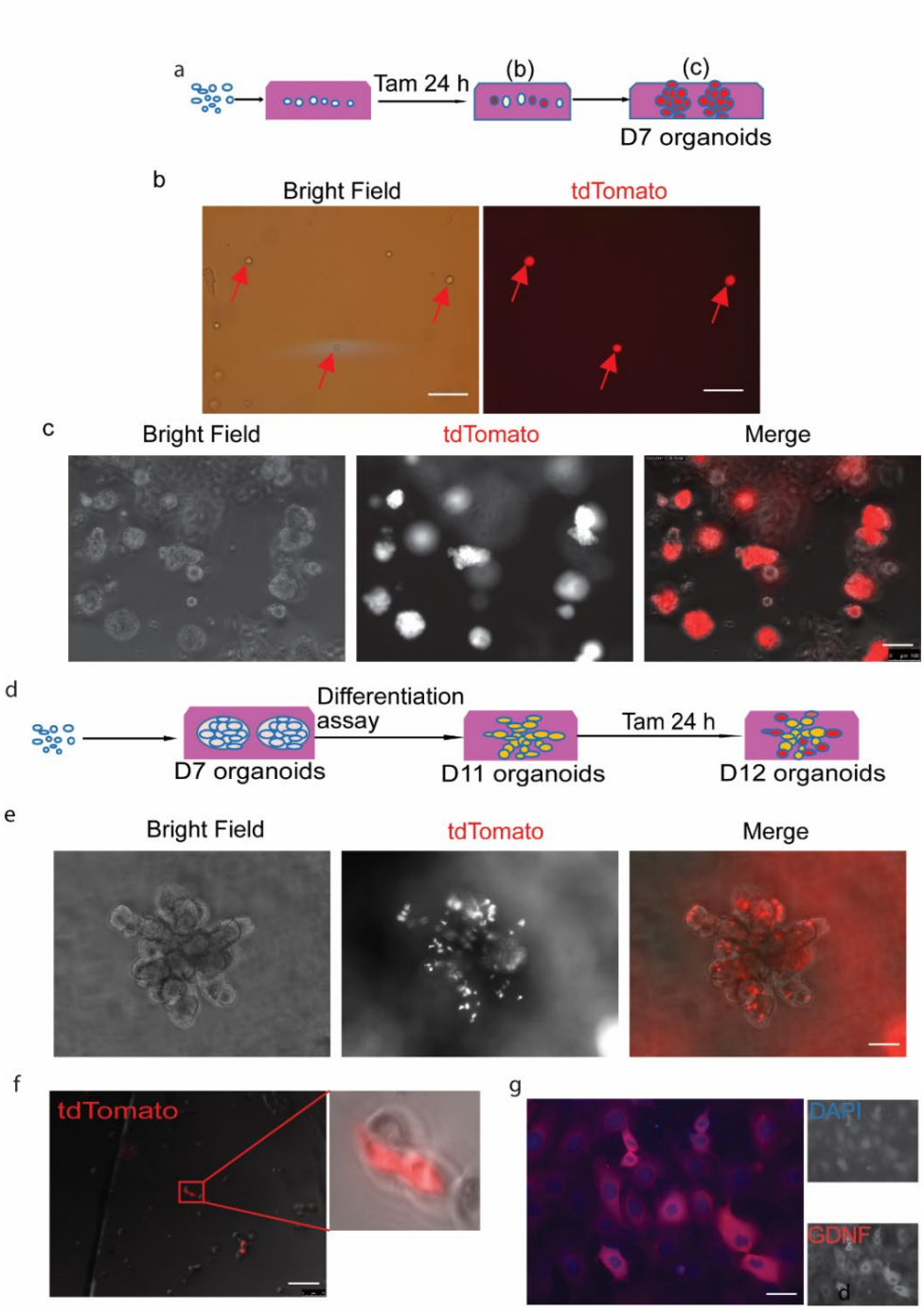
a
Tam 24 h
(b)
(c)
D7 organoids
b
Bright Field
tdTomato
c
Bright Field
tdTomato
Merge
d
Differentiation assay
Tam 24 h
D7 organoids
D11 organoids
D12 organoids
e
Bright Field
tdTomato
Merge
f
tdTomato
g
DAPI
GDNF

Supplementary Fig. 2 GDNF expression during cell proliferation in salivary gland organoids and 2D cultured cells. a) Schematic overview of the study design for experiments carried out in **b-*c***. Single cell were treated with 1 μM Tam for 24 h, after that the medium was refreshed. Organoids were analyzed at 7 days from the start of the culture. **b)** Representative images of single cells in Matrigel after 24 h Tam treatment. Scale bar=100 μm. **c)** Representative images of 7-day-old (D7) organoids after 24 h Tam treatment in culture. 80±2.83% organoids were red. Data represent mean ± SEM, Scale bar=100 μm. **d)** Schematic overview of the study design for experiments carried out in ***e***. D7 organoids were differentiated to budding organoids (D11 organoids) and subsequently treated with 1 μM Tam for 24 h and analyzed immediately after D12. **e)** Representative images of D12 budding organoids after 24 h Tam treatment in culture. Scale bar=100 μm. **f)** Representative live images of 2D cultured SG cells derived from GDNF$^{Cre\text{-}ERT2}$-tdTomato mice after 24 h Tam treatment. Scale bar=100 μm. **g)** GDNF IF staining of 2D cultured SG cells of GDNF$^{Cre\text{-}ERT2}$-tdtomato mice. Scale bar=25 μm. Pictures are representatives of 3 independent experiments.

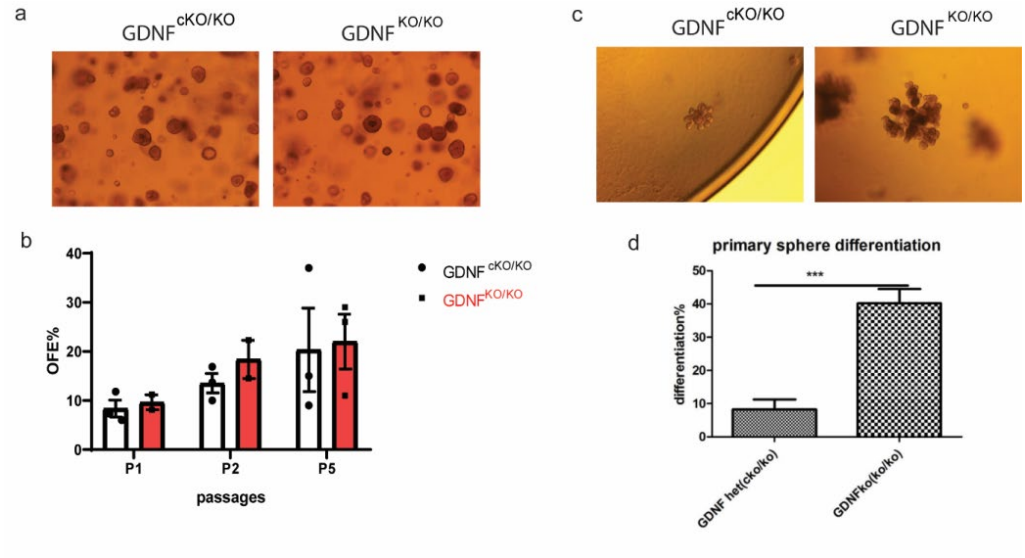

Supplementary Fig. 3 GDNF deficiency promote SGSC differentiation while has no effects on SGSC self-renewal capacity. $GDNF^{ko/ko}$ mice were established as described previously [48,49]. $GDNF^{ko/ko}$ mice do not survive after birth due to lack of the entire enteric nervous system and kidney agenesis. SGs were isolated from embryos and genotyping was performed to identify $GDNF^{cko/ko}$ (het) and $GDNF^{ko/ko}$(ko) embryos. **a)** Representative images of D7 organoids in culture derived from $GDNF^{cko/ko}$ (het) and $GDNF^{ko/ko}$(ko) embryos. **b)** Organoid formation efficiency (OFE%) of SGSCs derived from $GDNF^{cko/ko}$ (het) and $GDNF^{ko/ko}$ (ko) embryos in different passages. Data represent mean±SEM, N=3 embryos. **c)** Representative images of primary differentiation of organoids derived from $GDNF^{cko/ko}$ (het) and $GDNF^{ko/ko}$(ko) embryos. **d)** Primary sphere differentiation percentage were calculated by budding organoids relatively to the total number of seeded 5-day-old spheres in differentiation medium for 6 days. Mean ± SEM are shown, Student t-test. ***$p<0.001$. N=3 embryos.

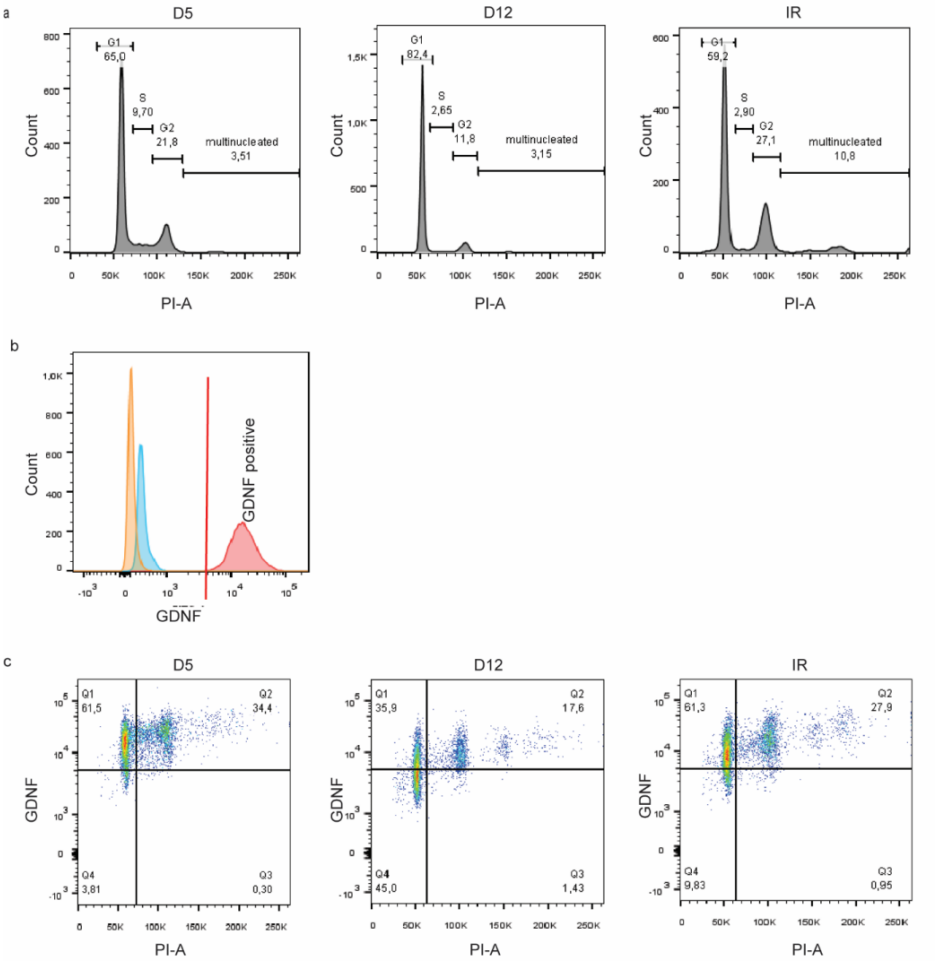

Supplementary Fig. 4 Analysis by flow cytometry of cell cycle and GDNF expression profiles. a) Representative cell cycle analysis of cells dissociated from D5, D12 and IR organoids after staining with PI. G0/G1, S, G2/M indicate the different cell cycle phases. Multinucleated refers to the cells that have more than 4N of DNA content. **b)** Detection of GDNF by flow cytometry in cells dissociated from D5, D12, and IR organoids. Cells was stained with anti-GDNF primary antibody and Alexa Fluor® 488 conjugated donkey anti-Rabbit secondary antibody (Red histogram) or blanc (Yellow histogram) or PI (Blue histogram). Red line showed the threshold that was used to gate the GDNF positive cells. **c)** Two parameter density plots of cells dissociated from D5, D12 and IR organoids after staining with GDNF (y-axis) and PI (x-axis). Cells were gated based on the threshold shown in panel b.

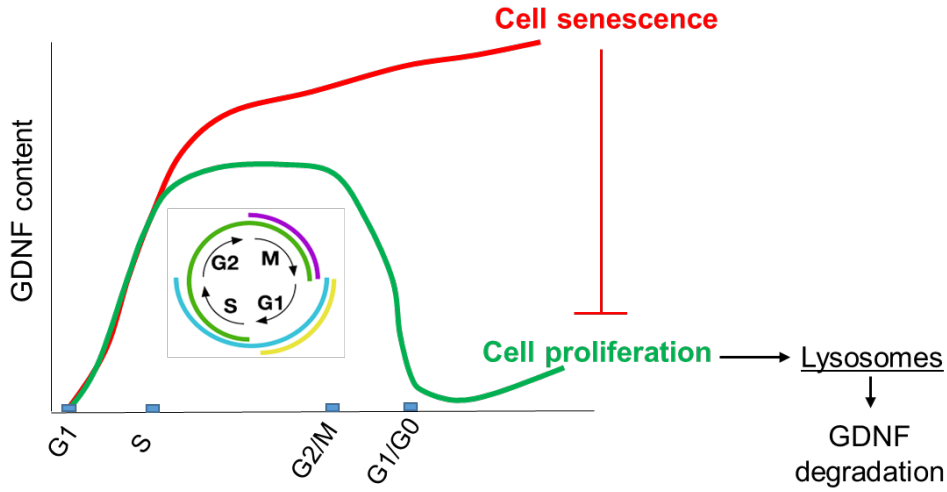

Supplementary Fig. 5 Proposed model of GDNF during cell proliferation and cellular senescence. GDNF dynamically changes during the cell cycle, while it accumulates in enlarged lysosomes after radiation-induced cell cycle arrest. We speculate that GDNF is not properly degraded after irradiation due to the dysfunction of the autophagy-lysosomal pathway.